

## Article

# Mechanistic Insights into Nonylphenol Stress on *BMP2* and *BMP4* Gene Expression in Red Crucian Carp (*Carassius auratus* Red var.)

Die Li <sup>1,†</sup>, Xiaojuan Cui <sup>1,†</sup>, Shuailin Chen <sup>1</sup>, Jia Xu <sup>1</sup>, Yujing Li <sup>1</sup>, Qiongyu Zhang <sup>2</sup> and Yuandong Sun <sup>1,\*</sup><sup>1</sup> School of Life and Health Sciences, Hunan University of Science and Technology, Xiangtan 411201, China<sup>2</sup> School of Fundamental Sciences, Yongzhou Vocational Technical College, Yongzhou 425100, China

\* Correspondence: syd@hnust.edu.cn; Tel.: +86-13786280789

† These authors contributed equally to the work.

**Abstract:** Nonylphenol (NP) is a known endocrine-disrupting chemical (EDC) that has been shown to affect bone development in mammals. However, the detrimental impacts of NP on the skeletal growth and development of aquatic species, especially bony fish, remain poorly understood. Bone morphogenic proteins (BMPs), essential for bone formation and osteoblast differentiation, act through the BMP-Smad signaling pathway. In this study, two *BMP* genes, *BMP2* and *BMP4*, were cloned and characterized in the red crucian carp (*Carassius auratus* red var.). The full-length cDNAs of *BMP2* and *BMP4* were 2029 bp and 2095 bp, respectively, encoding polypeptides of 411 and 433 amino acids, and share a typical TGF- $\beta$  domain with other BMPs. The tissue expression patterns of both genes were identified, showing ubiquitous expression across all studied tissues. Additionally, the exposure of embryos or adult fish to NP stress resulted in a downregulation of *BMP2*, *BMP4*, and other genes associated with the BMP-Smad signaling pathway. Moreover, the combined treatment of adult fish with NP and the specific BMP receptor inhibitor significantly reduced these genes' expression. These findings elucidate the mechanism of NP stress on *BMP2* and *BMP4*, suggesting a role for the BMP-Smad signaling pathway in the response to endocrine-disrupting chemicals in fish.

**Keywords:** Nonylphenol; endocrine-disrupting chemicals; BMPs; toxic effects; *Carassius auratus* red var.**Key Contribution:** This study suggests the crucial role of *BMP2* and *BMP4* in the adaptive responses of teleost fish to NP and highlights the significance of safeguarding aquatic ecosystems against EDC pollution.

**Citation:** Li, D.; Cui, X.; Chen, S.; Xu, J.; Li, Y.; Zhang, Q.; Sun, Y. Mechanistic Insights into Nonylphenol Stress on *BMP2* and *BMP4* Gene Expression in Red Crucian Carp (*Carassius auratus* red var.). *Fishes* **2024**, *9*, 159. <https://doi.org/10.3390/fishes9050159>

Academic Editor: Eric Hallerman

Received: 22 March 2024

Revised: 25 April 2024

Accepted: 25 April 2024

Published: 28 April 2024



**Copyright:** © 2024 by the authors. Licensee MDPI, Basel, Switzerland. This article is an open access article distributed under the terms and conditions of the Creative Commons Attribution (CC BY) license (<https://creativecommons.org/licenses/by/4.0/>).

## 1. Introduction

Nonylphenol (NP), a prominent endocrine-disrupting chemical (EDC) and the primary degradation product of alkylphenol ethoxylates, exhibits estrogenic activity in a variety of wildlife species [1]. Widespread in industrial applications and consumer products, human and animal exposure to NP occurs through multiple routes, including latex coatings, adhesives, paper products, detergents, and cosmetics [2]. Research on mammals has revealed that perinatal exposure to NP can affect brain function [3], cardiac function [4], and bone development [5] in the offspring of exposed individuals. In particular, the impact of NP on bone development has been well established. For instance, exposure to NP significantly compromises bone integrity by affecting osteoblasts and osteoclasts, which are vital for the formation and homeostasis of bone tissue [6,7]. Additionally, NP may contribute to abnormal skeletal development by interfering with critical signaling pathways, such as *Wingless/Int-1* (*Wnt*) and  $\beta$ -catenin, either directly or indirectly, thereby disrupting the normal processes of skeletal growth and maturation [8]. NP also exerts toxic effects on aquatic organisms, resulting in multi-organ damage [9–11]. It has been shown that exposure to NP is correlated with the development of skeletal abnormalities in fish embryos.

Abnormalities were observed in developing Asian stinging catfish (*Heteropneustes fossilis*) larvae exposed to NP 5 h after hatching in [12]. In zebrafish (*Danio rerio*), 24 h of embryonic exposure to NP resulted in the observation of tail skeletal malformations in [13]. Similarly, in goldfish (*Carassius auratus*), early blastula-stage embryos were exposed to NP and exhibited skeletal malformations between 24 and 72 h after fertilization following exposure to varying concentrations of NP in [14].

During skeletal development, the majority of the bones in the body are established by the endochondral bone formation process [15]. Chondrocyte maturation and the endochondral bone development process are tightly regulated by a series of growth factors and transcription factors, including bone morphogenetic proteins (BMPs), which play a crucial role [16]. BMPs activate the BMP-Smad signaling pathway, which is essential for osteogenesis, skeletal development, and bone formation [17]. Specifically, BMP2 and BMP4 act as secreted ligands that engage serine–threonine kinase-type II receptors, leading to the activation of type I receptors and the subsequent phosphorylation of Smad proteins. This cascade regulates the expression of key bone formation markers such as runt-related transcription factor 2 (Runx2) and Osterix [18]. Multiple endocrine-disrupting chemicals (EDCs), such as bisphenol A (BPA) [19] and polychlorinated biphenyls (PCBs) [20], have been shown to interfere with bone development by inhibiting genes associated with the BMP-Smad pathway. Studies of various mammalian species, including mice [21], pigs [22], and goats [23], have highlighted the significant role of BMP2 and BMP4 in bone development. Additionally, extensive research has been conducted on BMP2 and BMP4 in various fish species. The cDNA sequences of *BMP2* and *BMP4* have been identified in early investigations focusing on zebrafish (*Danio rerio*) [24] and Japanese flounder (*Paralichthys olivaceus*) [25]. Subsequently, studies delving into the expression of *BMP2* were carried out on Jian carp (*Cyprinus carpio* var. Jian) [26] and barbel steed (*Hemibarbus labeo*) [27]. Similarly, *BMP4* expression studies were conducted on mandarin fish (*Siniperca chuatsi*) [28], providing further insights into the significance of *BMP2* and *BMP4* in fish skeletal development.

*Carassius auratus* red var. accounts for an important proportion of freshwater aquaculture production worldwide, but it is susceptible to various factors during production [29]. A previous study by our research group showed that NP affects *C. auratus* red var. and leads to the development of abnormal skeletons [30]; however, the molecular mechanism of NP's effect on the skeletal development of *C. auratus* red var. remains unclear. BMPs act as the key genes of the BMP-Smad pathway, which are known to be involved in the regulation of skeletal development. In the present study, two key members of the BMP family (*BMP2* and *BMP4*) were successfully cloned and characterized from *C. auratus* red var. The expression levels of the *BMP2* and *BMP4* transcripts in different tissues were analyzed by real-time fluorescence quantitative PCR (qRT-PCR). Furthermore, the temporal patterns of *BMP2* and *BMP4* in response to NP exposure were investigated in embryos and adult fish. The results of this study can help broaden the understanding of the roles of the BMP-Smad pathway in response to environmental endocrine disruptors.

## 2. Materials and Methods

### 2.1. Fish and Sampling

Two-year-old healthy *C. auratus* red var. were obtained from the Engineering Research Center of Polyploid Fish Breeding and Reproduction of the State Education Ministry at Hunan Normal University. The fish were acclimatized in an indoor freshwater tank at  $25 \pm 1$  °C and fed a commercial diet (crude protein, 32.2%; crude lipid, 6.5%; ash, 10.4%; and gross energy, 18.5 MJ/kg) twice daily at 9:00 and 16:00 for one week. After no abnormal symptoms were observed, the *C. auratus* red var. fish were subjected to further study.

Three healthy fish were sacrificed as one group, and samples from the gill (G), caudal fin (C), heart (H), intestine (I), kidney (K), liver (L), muscle (M), brain (B), and spleen (S) were collected. All samples were immediately homogenized in TRIzol reagent (Invitrogen, Carlsbad, CA, USA) and stored at  $-80$  °C until needed for RNA extraction for cloning and the detection of tissue differential expression in *BMP2* and *BMP4* genes.

## 2.2. NP Treatments of Embryos

A previous study by our research group found that the embryos of *C. auratus* red var. treated with 3  $\mu\text{mol/L}$  of NP exhibited relatively obvious skeletal malformations, and the mortality rate was low [30]. Therefore, 3  $\mu\text{mol/L}$  NP was selected as the experimental concentration. The eggs and sperm from three sexually mature male and female *C. auratus* red var. were artificially fertilized using the semi-dry method. The fertilized eggs were then placed in a 25 cm sterile, dry Petri dish containing aerated water for incubation. After fertilization for 2 min, all the embryos were exposed to NP with concentrations of 0  $\mu\text{mol/L}$  (blank control, 0.01% ethanol) or 3  $\mu\text{mol/L}$ . Each treatment group was employed for 5 parallel replicates (5 Petri dishes), with approximately 300 embryos in each Petri dish. Embryo incubation and NP exposure were carried out in the plates at  $25 \pm 1$  °C. The water was changed approximately every 4 h. Intact embryos were collected at six stages: 6 hpf (hours post-fertilization), 12 hpf, 24 hpf, 48 hpf, 72 hpf, and 96 hpf. From each group, we collected 3 tubes of 30 embryos per tube from 5 Petri dishes, for a total of 6 tubes at each time point (Table S1). We used liquid nitrogen to stop embryo development and then stored the samples at  $-80$  °C until RNA extraction.

## 2.3. NP Exposure and Inhibitor Intraperitoneal Injection of Adult Fish

Before the initiation of the study, all fish were acclimatized to laboratory conditions for a week. For NP exposure, *C. auratus* red var. fish (approximately 50 g in weight) were divided into three groups randomly. Each group had three replicates with 15 fish. Three identical round fiberglass tanks (200 L) were used to rear the fish ( $n = 15$  per tank), with continuous aeration. The rearing conditions were as follows: water temperature was  $25 \pm 1$  °C, dissolved oxygen was higher than 5 mg/L, the concentration of ammonia nitrogen was  $<0.5$  mg/kg, and pH was maintained at 6.5–7.5. The experimental water was tap water after aeration for 3 days. Adult fish in the experimental groups were exposed to NP at concentrations of 251.3  $\mu\text{g/L}$  or 753.9  $\mu\text{g/L}$  dissolved in ethanol. The control group was treated with an equal concentration of ethanol in the tanks (0.01% ethanol, *v/v*). The exposure was conducted using a semi-static water system, where half of the water was replaced daily, and then, the reagent was added to maintain the original concentration. The selected NP concentrations were based on the 96 h LC<sub>50</sub> value for *C. auratus* red var., which is 251.3  $\mu\text{g/L}$  [31]. Three fish from each group were sampled randomly at 12, 24, 48, 72, and 96 h post-exposure to NP. The caudal fin of *C. auratus* red var. at each time point was collected, frozen immediately in liquid nitrogen, and stored at  $-80$  °C until RNA isolation.

For the combination treatment with the BMPRI-specific inhibitor LDN193189 and NP, *C. auratus* red var. fish were selected ( $n = 12$ ) and randomly divided into four groups. Experiments were carried out in a 50 L round fiberglass tank. The four groups were divided into control, LDN193189, NP, and NP + LDN193189 treatments. The experimental conditions and the experimental water were the same as those used in the previously described NP exposure experiment. Each fish received an intraperitoneal injection of 200  $\mu\text{L}$  of the respective treatment, with three replicates per group. Both the control and NP groups were injected with 0.01% dimethyl sulfoxide (DMSO), while the LDN193189 and NP + LDN193189 groups received LDN193189 at a dose of 0.625 mg/kg body weight, freshly prepared in dimethyl sulfoxide. This dose was based on the effective dose used in a previous study with sailfin molly (*Poecilia latipinna*) [32]. At 12 h after injection, the control and LDN193189 groups were exposed to 0.01% ethanol, whereas the NP and NP + LDN193189 groups were exposed to a concentration of 251.3  $\mu\text{g/L}$  NP. Samples of the caudal fin were collected from 12 live fish at 48 h post-exposure. Fish were not fed throughout the entire exposure process.

## 2.4. RNA Extraction

Total RNA from the collected samples was extracted individually with Trizol reagent under RNase-free conditions. RNA purity was estimated using a nucleic acid protein

analyzer (BioPhotometer Eppendorf, Hamburg, Germany) based on the A260/A280 ratio, and the quality was assessed by electrophoresis on a 1.0% agarose gel.

## 2.5. Cloning the cDNA Sequence of BMP2 and BMP4

All primers (Table 1) were designed using the Primer Premier 5 software (<https://www.premierbiosoft.com/primerdesign/index.html> (accessed on 5 July 2022)) and synthesized by the Sangon Biotech Co., Ltd. (Shanghai, China). To amplify partial cDNA fragments of BMP2 and BMP4 in *C. auratus* red var., degenerate primers of *C. auratus* red var. BMP2 were designed from homologous regions of the BMP2 sequences of other teleosts (GenBank accession no. AB265811.1), and degenerate primers of BMP4 were designed from homologous regions of the BMP4 sequences of other teleosts (GenBank accession no. AB874478.1). The PCR template for the BMP2/BMP4 genes was, respectively, synthesized from 1 µg of brain and intestine RNA of *C. auratus* red var. with a PrimeScript™ 1st Strand cDNA Synthesis Kit (Takara, Kusatsu, Japan) according to the manufacturer's instructions. PCR was performed in a total reaction volume of 20 µL containing 2 µL of 10× LA Taq Buffer II (Mg<sup>2+</sup> plus), 1 µL of cDNA template, 2 µL of dNTP mixture (2.5 mM each), 0.5 µL of each primer (10 µM), 13.8 µL of ddH<sub>2</sub>O, and 0.2 µL of LA-Taq DNA Polymerase (Takara, Kusatsu, Japan). The PCR conditions were 94 °C for 1 min; 35 cycles of 30 s at 98 °C; and 1 min 10 s at 61 °C, followed by a final extension for 10 min at 72 °C. The PCR products were purified using the Agarose Gel DNA Purification Kit (Accurate Biotech Co., Ltd., Changsha, China) and were inserted into the pMD18-T vector using a TA cloning kit (Accurate Biotech Co., Ltd., Changsha, China). The recombinant plasmid vector was transformed into *Escherichia coli* DH5α competent cells (Accurate Biotech Co., Ltd., Changsha, China). The positive clones were sequenced by Beijing Tsingke Biotechnology Co., Ltd. (Beijing, China), and the results were verified by the BLAST program (<https://blast.ncbi.nlm.nih.gov/Blast.cgi> (accessed on 12 September 2022)). All the PCRs in this study were repeated, and the results were consistent.

**Table 1.** The sequences of primers used in this study.

Primer Names	Sequence (5' to 3')	Application
BMP2-F	GCTGTTGCTCGGTCAGGTGT	Partial sequence obtaining
BMP2-R	CAGCCCTCCACCACCATGT	Partial sequence obtaining
BMP4-F	GAAGGGAAGAAGAAAGCGTCG	Partial sequence obtaining
BMP4-R	GACCTCTTTGCTTCGGGGCTG	Partial sequence obtaining
BMP2-5'GSP	GTGGAGCACCTCAACCAGAAGCCCG	5'-RACE PCR
BMP2-3'GSP	AGCATGGCCCCTTCCAAAGAGCCTC	3'-RACE PCR
BMP4-5'GSP	CTCCCGTGGGTTGGGGATCTGAGAC	5'-RACE PCR
BMP4-3'GSP	CGAGTCGAGCGAACACCGTGAGAGG	3'-RACE PCR
BMP2-5'NGSP	AGCCCGTGGTTGTGCTGGGATTTCGC	Nested 5'-RACE PCR
BMP2-3'NGSP	TGTTTCAGGCCAGCATGGCCCCTTCC	Nested 3'-RACE PCR
BMP4-5'NGSP	TGGGGATCTGAGACTGCATCATCTATCT	Nested 5'-RACE PCR
BMP4-3'NGSP	CACCGTGAGAGGATTCCATCATGAAGAG	Nested 3'-RACE PCR
BMP2-QF	GCGATCCGATATTAACCTTCCTG	qRT-PCR
BMP2-QR	GCTTTCCCATAGTGCTCCTTG	qRT-PCR
BMP4-QF	TGAACTGCTGCGGGACTTTG	qRT-PCR
BMP4-QR	GACTCGTGGACCTCTCGGGAT	qRT-PCR
Runx2-QF	CACAGAGCCATAAAGGTCACGG	qRT-PCR
Runx2-QR	GGAGTTGGGGTTGCTAAGCG	qRT-PCR
Osterix-QF	CAAACCCGTCCCATTCTCTG	qRT-PCR
Osterix-QR	GCACCAAGCCTCTCCAACCTC	qRT-PCR
BMPRI-QF	TGGCGTACTCTGCAGCCTGT	qRT-PCR
BMPRI-QR	TGGGATGTCCACTTCATTTGTG	qRT-PCR
β-actin-QF	TCCCTTGCTCCTTCCACCA	qRT-PCR
β-actin-QR	GGAAGGGCCAGACTCATCGTA	qRT-PCR

To obtain the 5' and 3' ends of each cDNA, a number of gene-specific primers (Table 1) were designed for the target genes to replicate sense or antisense regions of their amplified partial fragments, sequenced above. 5'-RACE and 3'-RACE were performed with the RACE cDNA Amplification Kit (Vazyme Biotech Co., Ltd., Nanjing, China) using brain or intestine

RNA following the manufacturer's instructions. Nested 5'- and 3'-RACE PCR products of the expected size were handled and sequenced as described above. The full-length cDNAs of the target genes were assembled by aligning the partial cDNA fragments and the 5'- and 3'-RACE fragments with the aid of the ContigExpress program in the Vector NTI Advance 11 sequence analysis software packages (Invitrogen).

## 2.6. Sequence Identification of BMP2 and BMP4

The ORF finder program (<https://www.ncbi.nlm.nih.gov/orffinder/> (accessed on 5 April 2023)) and ExpASy (<http://web.expasy.org/translate/> (accessed on 5 April 2023)) were used to deduce the amino acid sequences of BMP2/BMP4. The BLASTX and BLASTP programs (<http://blast.ncbi.nlm.nih.gov/Blast.cgi> (accessed on 11 April 2023)) were used to analyze the nucleotide and deduced protein sequences, respectively. The isoelectric point (pI) and molecular weight (Mw) were calculated by the pI/Mw tool ([http://www.expasy.ch/tools/pi\\_tool.html](http://www.expasy.ch/tools/pi_tool.html) (accessed on 11 April 2023)). The protein motif features were predicted by the Simple Modular Architecture Research Tool (<http://smart.cmbi-heidelberg.de/> (accessed on 11 April 2023)). The BMP2 and BMP4 amino acid sequences of other vertebrates were searched in the NCBI protein database, and the GenBank accession numbers are listed in Table 2. Multiple sequence alignment of BMP2 and BMP4 was performed with the MegAlign (<https://www.dnastar.com/software/lasergene/megalign-pro/> (accessed on 3 June 2023)) and GeneDoc (<https://nrbsc.org/gfx/genedoc/> (accessed on 3 June 2023)) programs, and the identity was analyzed by the NCBI BLASTP program. Phylogenetic analysis was constructed using the neighbor-joining (NJ) method implemented in the MEGA 5.0 package (<http://www.megasoftware.net/> (accessed on 3 June 2023)) based on sequence alignment using the Clustal W method with 1000 bootstrap replicates.

**Table 2.** Amino acids used to construct the phylogenetic tree of the BMP2/BMP4 genes.

Protein Name	GenBank Access. No.
<i>Carassius auratus red variety</i> BMP2	PP411940
<i>Carassius auratus</i> BMP2	BAN17326.1
<i>Danio rerio</i> BMP2	AAI14257.1
<i>Cyprinus carpio</i> BMP2	XP_042602743.1
<i>Megalops cyprinoides</i> BMP2	XP_036398004.1
<i>Anguilla Anguilla</i> BMP2	XP_035277091.1
<i>Astyanax mexicanus</i> BMP2	KAG9268738.1
<i>Puntigrus tetrazona</i> BMP2	XP_043074619.1
<i>Sinocyclocheilus anshuiensis</i> BMP2	XP_016337425.1
<i>Anabarrilius grahami</i> BMP2	ROL52452.1
<i>Salmo trutta</i> BMP2	XP_029587557.1
<i>Homo sapiens</i> BMP2	ACV32596.1
<i>Mus musculus</i> BMP2	AAI00345.1
<i>Gorilla gorilla gorilla</i> BMP2	XP_004061840.1
<i>Bos taurus</i> BMP2	AAI42130.1
<i>Gallus gallus</i> BMP2	NP_001385099.1
<i>Columba livia</i> BMP2	XP_021150021.1
<i>Carassius auratus red variety</i> BMP4	PP411941
<i>Carassius auratus</i> BMP4	XP_026085110.1
<i>Cyprinus carpio</i> BMP4	XP_042630442.1
<i>Sinocyclocheilus rhinoceros</i> BMP4	XP_016424235.1
<i>Puntigrus tetrazona</i> BMP4	XP_043118272.1
<i>Danio rerio</i> BMP4	NP_571417.1
<i>Salmo salar</i> BMP4	XP_014066471.1
<i>Sparus aurata</i> BMP4	XP_030298905.1
<i>Homo sapiens</i> BMP4	NP_001334843.1
<i>Mus musculus</i> BMP4	AAH13459.1
<i>Gorilla gorilla gorilla</i> BMP4	XP_030857865.1
<i>Gallus gallus</i> BMP4	NP_990568.4
<i>Bos taurus</i> BMP4	NP_001039342.1
<i>Columba livia</i> BMP4	XP_005510342.1
<i>Xenopus laevis</i> BMP4	NP_001081501.1

## 2.7. Gene Expression Analysis by RT-qPCR

Total RNA was reverse-transcribed into cDNA using the HiScript II Q RT SuperMix for qPCR (+gDNA wiper) kit (Vazyme Biotech Co., Ltd., Nanjing, China), and the cDNA was diluted five times for a quantitative template. Gene-specific primers for quantitative real-time PCR (qRT-PCR) were designed to determine the mRNA expression levels of *BMP2*, *BMP4*,

*Runx2*, *Osterix*, and *BMPRI* in various samples (Table 2). *C. auratus* red var.  $\beta$ -actin was used as an internal control to verify successful transcription and to calibrate the cDNA template for corresponding samples. qRT-PCR was carried out on the Quant-Studio™ 3 Real-Time PCR System (Thermo Fisher, Waltham, MA, USA) in a total volume of 20  $\mu$ L, containing 1  $\mu$ L of cDNA template, 0.3  $\mu$ L of each primer (10  $\mu$ M), 10  $\mu$ L of 2 $\times$  ChamQ Universal SYBR qPCR Master Mix (Vazyme Biotech Co., Ltd., Nanjing, China), and 8.4  $\mu$ L of RNase-Free ddH<sub>2</sub>O. The PCR cycling procedure was as follows: initial denaturation at 95 °C for 30 s, followed by 40 cycles of amplification at 95 °C for 10 s and 60 °C for 30 s; a melting curve was obtained at the end of the reaction, and a single peak was observed, demonstrating the absence of dimeric primers or the generation of non-specific amplification. Relative expression levels were calculated by the  $2^{-\Delta\Delta C_t}$  method.

### 2.8. Statistical Analysis

Data obtained from qRT-PCR were expressed as mean  $\pm$  SEM ( $n = 3$ ) and were analyzed with the SPSS 26.0 software (Chicago, IL, USA). Differences between means were assessed by one-way analysis of variance (ANOVA) followed by Duncan's multiple comparison tests. Differences were considered significant when  $p < 0.05$ . Relative expressions of the *BMP2* and *BMP4* genes were plotted using the GraphPad Prism 8.0 software (San Diego, CA, USA).

## 3. Results

### 3.1. Cloning and Sequence Characteristics of *BMP2* and *BMP4* cDNA

The full length of *BMP2* cDNA that we isolated from *C. auratus* red var. was 2029 bp, which contained a 5'-untranslated region (UTR) of 375 bp, a 1236-bp open reading frame (ORF), and a 418 bp 3'-UTR with a 31 bp polyA tail. The ORF encoded a 411-amino-acid peptide with a predicted molecular weight of 46.97 kDa and a theoretical isoelectric point of 7.72 (Figure 1A). The complete cDNA sequence of *BMP4* was 2095 bp, and the predicted ORF was 1302 bp, encoding a protein with 433 amino acids. It included a 359 bp 5'-UTR and a 434 bp 3'-UTR with a 26bp polyA tail (Figure 1B). The calculated molecular mass and theoretical isoelectric point of *BMP4* were 49.56 kDa and 8.56, respectively. The sequences of *BMP2* and *BMP4* were submitted to NCBI GenBank, and the accession numbers are listed in Table 2. Domain architecture analysis of *BMP2*/*BMP4* revealed three conserved and key structural features, including a signal peptide, a TGF- $\beta$  propeptide, and a mature TGF- $\beta$  domain (Figure 2).

### 3.2. Homology and Phylogenetic Analysis

Multiple sequence alignments of *BMP2* and *BMP4* are presented in Figures 3 and 4, respectively, showing their homology at the protein level. *BMP2* exhibited the highest homology with *BMP2* from other cyprinids including goldfish (*Carassius auratus*) (BAN17326.1), sharing 98.30% sequence identity. It also showed significant homology with blind cavefish (*Sinocyclocheilus anshuiensis*) (XP\_016337425.1), common carp (*Cyprinus carpio*) (XP\_042602743.1), and tiger barb (*Puntigrus tetrazona*) (XP\_043074619.1), and the sequence identity was about 93%. Similarly, *C. auratus* red var. *BMP4* shared the highest homology with *C. auratus* (XP\_026085110.1), and sequence identity was 98.21%. It has higher homology with *C. carpio* (XP\_042630442.1), *S. anshuiensis* (XP\_016424235.1), and *P. tetrazona* (XP\_043118272.1), and the sequence identities were 96.43%, 94.90%, and 93.89%, respectively.

The phylogenetic analysis in Figure 5A revealed that the *BMP2* sequences formed two distinct branches, one representing bony fish, while the other was the branch of birds and mammals, indicating a closer relationship between *C. auratus* red var. *BMP2* and *C. auratus* *BMP2*. The phylogenetic tree of *BMP4* encompassed sequences from various species, including fish, amphibians, birds, and mammals, while *C. auratus* red var. *BMP4* had the highest homology with *C. auratus* *BMP4* (Figure 5B). These relationships depicted in the phylogenetic tree align well with traditional taxonomic affinities.

# A

```
1 gctccaatcaatggcacagacggcagcctgctgcaagcagagatgagtctccaagcagc-
61 ctctgaaaacttctactgatcagaatTTTTAGGCGAAAAATGACAGATCCAGGACTTTGC
121 gaactcgcgctgctcaactcttgggaattgctggTTTTCTTGACCTAAGCATTGGCCTTC
181 attagagttaactgcagtttagtttgaagtgttgcTCAAGTATGAACAAGAAGAGGAGAC
241 ctgagttgCGGCGACTCTCTGCTGTTGGGATAAAAAAATCGCTTGTGGATTAACAAC
301 gaattcatgtggaatttaagagacgacgggacgcagaccggccacagcgttctctctt
1 M V D V V R T L T V L L L G Q
361 cggaactgactgatcATGGTCGACGTGGTCCGCACTCTCACGGTGTGTTGCTCGGTCAG
16 V L L G S T T G L I P E I D Q R K Y S D
421 GTGTTGCTGGGAAGTACCCTGGACTCATTCCAGAGATCGACCAACGAAATACAGTGAT
36 S G R H P P E R S D I N F L K E F E L R
481 TCAGGGAGACACCCCGCGGAGCGATCCGATATTAACTTCCTGAAGAGTTTGAGCTACGG
56 L L N V F G L K R K P M P S K S A V V P
541 CTGCTCAACGTGTTTGGACTGAAGCGAAAACCCATGCCGAGCAATCGGCAGTGGTCCCT
76 Q Y M L D L Y Y M H S E N D D P N I R R
601 CAGTACATGCTGGACTTGTATTATATGCACTCAGAAAATGATGACCCGAACTCCGGCGC
96 P R S T M G K H V E R A A S R A N T I R
661 CCAAGGAGCACTATGGGAAGCATGTGGAACGGGCGGCGAGCAGCAACACACATAACGA
116 S F H H E E A L E A L S S L K G K T T Q
721 AGTTTTTCATCATGAAGAGGCTCTCGAGGCCTCTCCAGCTGAAAGGAAAACCAACGCAG
136 Q F F F N L T S V P A E E L I T A A E L
781 CAGTTTTTCTTCAACCTTACCTCCGTTCTCGCGAGGAGTGATCACGGCAGGGAGCTG
156 R I F R D Q V L G D T G A S G Y H R I N
841 CGCATTTTCAGGGACCAGTTCTCGGTGACACTGGTCAAGTGGTTACCACCGAATTAAT
176 I Y E V F R P A L A P S T E P L T R L L
901 ATTTACGAGGTGTTGAGCCAGCCCTGGCCCTTCCACAGAGCTCTTACCAGACTTCTC
196 D T R L V Q D S H T R W E S F D V G S A
961 GACACCCGCTGTTGTCAGGACTCTCATACTCGCTGGGAGAGCTTIGATGTGGGTTCCGCA
216 V A R W A H E S L H N H G L L V E V L H
1021 GTGGCTCGCTGGGCCATGAATCCCTGCATAACCATGGGCTCCTGGTGGAGGTGCTCCAT
236 P E E S E G S A E V E R N R R H V R V
1081 CCCGAAGAGTCGGGAAGGATCCGCGGAGTTGAGAGAAAACCGGAGGAGCAACGTAAGGTT
256 S R S L H A D E D S W V Q A R P L L V T
1141 AGTCGCTCCCTTCATGCGGACGAGGACTCGTGGGTGACGGCCGACCCCTGCTAGTGACC
276 Y S H D G Q G S A V L N S N R E K R Q V
1201 TACAGCCATGACGGTCAGGGCTCCGCGTCTTAATTCAACAGAGAGAAGCGGCAGGTG
296 R Q R P K Q R R K Q Q Q R T N C R R H A
1261 CGGCAAGGCCGAGCAGCGCAGGAAGCAGCAACAGCCACAACTGCAGGCGGCAGCCT
316 L Y V D F S D V G W N E W I V A P P G Y
1321 CTCTACGTGGACTTCAGCGAGTGGGCTGGAACGAGTGGATTGTGGCGCCACCCGGCTAC
336 H A F Y C Q G E C P F P L S D H L N S T
1381 CATGCTTTCTACTGTCAGGGCGAGTGTCCCTTCCGCTGTCCGACCACCTGAACTCCACC
356 N H A I V Q T L V N S V N S N I P K A C
1441 AATCAGCCATCGTCCAGACGCTGGTGAACCTCGGTCAATTCCAATATCCCAAGCGTGT
376 C V P T E L S P I S L L Y L D E Y E K V
1501 TGCCTCCCAACAGAGCTTAGTCCCATATCGCTGCTATACCTGGACGAGTACGAGAAAGTC
396 I L K N Y Q D M V V E G C G C R *
1561 ATTCTTAAAACTACCAAGACATGGTGGTGGAGGGCTGCGGGTCCGATGGgaactacat
1621 ctccccaatgaagacttttatttatacaaaaagatcgttcaaaagagctattttggaggaag
1681 aaaagaaatataatgaatataatatttattggtgactgaaaaaatgggaaaaataatatttt
1741 aatgagagtgcttcttttctgagtgctttgaaagatgtttttttctctgccccatgtg
1801 catttcaaaaataagtgaattgcccatgaagtataatgctcagattttttatgatgtattt
1861 attgcataaccctttatttgaatgatgggtatttcatcatgagaaaaatataatgatc
1921 ttcatttagtgcatccatttttgaaccccccaaaaataaacatgggatgaagttttctt
1981 taaagttcatgatataacaaaaaaaaaaaaaaaaaaaaaaaaaaaaaaaaaaaaa4
```

Figure 1. Cont.

B

```

1 ggagaactggatgctgggttcagacgggtgatgtcctccgtgctcgactcttctctggagata↓
61 cacagatccgcgttcgcatgggactcttttggcttctctctacgtgatgcggaactaatga↓
121 tctaaacattcgcttagggttgacttttctgtctgaggtgaactcctttaaactc↓
181 cttttaccgtcttctcatccaggaataccgcgcgcatctctaccaatggaaggaatct↓
241 ccccgctgttgttaaacagccttccaggagcaagtaaacattcactcgaggaactcgtcct↓
1
301 ggatcagctctcgacaaaacatggactgttttcccatgctttatcttctgtcgagacatc↓
2 IPGNRMPMLVLLLCQVLLGES
361 TGATTCCCTGGTAATCGAATGCCGATGGTCCCTTTATTATGCCAAGTCTACTGGGAGAGA↓
22 SYASLIP E E G K K K A S A Q H L G
421 GCAGCTATGCTAGTCTAATACTGAGGAAGGGAAGAAAGCGTCGGCTCAGCACCTGG↓
42 Q S H E L L R D F E A T L L H M F G L Q
481 GTCAGAGTCATGAACCTGCTGCGGGACTTTGAAGCCACGCTGCTGCACATGTTTGGGCTGC↓
62 R R P R P S Y S A V V P Q Y L L D L Y R
541 AGAGGCGACCGCGACCCAGCTACTCGGCTGTGGTGCQCCOCCATCTGCTGGACCTGATC↓
82 L Q S G E A E E A G A H D V S F H Y P E
601 GCCTGCAGTCAGGGGAGGCCGAAGAGGCCGGGGCCACGACGTGAGCTTCCATTATCCCG↓
102 R S T S R A N T V R G F H H E H M E E
661 AGAGGTCCACGAGTCGAGCGAATCCCGTGTGAGAGATTCCATCATGAAGAGCAGTAGATG↓
122 L Q S D G S E T P L R F V F N L S S I P
721 AGCTGCAGTCAGACGGCTCTGAGACTCCOCCACGCTTTCGTTCAATCTCAGCAGCATCC↓
142 E E E L I S T A E L R L Y R K Q I D D A
781 CAGAGGAGGAACCTATTCTACCGCAGAGCTTCGCTCTCAGGAAACAGATAGATG↓
162 I S D P Q P T G D E G L H R I N I Y E V
841 CAATCTCAGATCCCAACCCACGGGAGACGAAAGTCTACACAGGATAAACATATACAGG↓
182 L K P P R A G Q L I T Q L L D T R L V R
901 TGCTGAAGCCCCCGCGGGCCGGACAGCTCATCACACAGCTGCTGGACACTCGACTGGTGC↓
202 H N T T R W E S F D V S P A V L R W T R
961 GCCACAACAGACTCGATGGGAGAGCTTCGACGTGAGTCCGGCCGTGCTGCGCTGGACCC↓
222 D K S S N H G L A V E V V P L N R T S R
1021 GTGACAAGAGCTCCAATCACGCCCTGGCTGTGGAGGTGGTGCCTGAACCGAACCTGC↓
242 H Q G R H V R V S R S L H P L P D A D W
1081 GTCACCAGGGACGCCACGTACCGCTCAGTCTCCTTGCATCCGCTTCCCGACGCAGACT↓
262 S Q L R P L L V T E G H D G K S H P L T
1141 GGAGCCAGCTTCGCCCCCTGCTGGTTCAGGTTGGACACGACGGAAAGTCAACCCCTGA↓
282 R R A K R S P K Q R G R K R N R N C R E
1201 CGCGGCGAGCGAAGCGCAGCCCGAAGCAAGAGGTCCGCAAGCGCAACCGAACTGTGGC↓
302 N A L Y V D F S D V G W N D W I V A P E
1261 GACACGCGCTTATGTGGACTTCAGTGTGTTGGCTGGAACGACTGGATCGTGGCGCCG↓
322 E Y Q A Y V C H G E C F F P L A D H L E
1321 CCGGATATCAGGCGTACTACTGTCACGGGAGTGTCCGTTCCCTTTGGCCGATCACCTGA↓
342 E T N H A I V Q T L V N S V N T N I P E
1381 ACTCCACCAATCACGCTATTGTGTCAGACGCTGGTGAACCTGGTGAACACCAATATCCCA↓
362 A C C V E T E L S A T S M L Y L D E T G
1441 AGGCCITGCTCGTTCACACAGAGCTCAGTGCCTCTCCATGCTCTACCTGGACGAGACGG↓
382 F G W V L K N Y Q E E W W W G K R M C A
1501 GAACAGGGTGGGTGCTGAAGAACTATCAGGAGAGGTGGTGGTGGGGAAGAGGATGTGT↓
402 A A D R D T A T P W T L I Y N I W V L G
1561 CTGCCGCTGACCGGGACACAGCTACACCCTGGACACTTATTTATAACATCTGGGCTTGG↓
422 R C V F L V S S I H I F *
1621 GAAGATGTGTGTTTCTTGTCTCCTCGATACATATATTTTGAcaaaaaaagtatatataaa↓
1681 tatatatttatatacaacataattaaacaaaaaaaccgctcttattttaattatagtca↓
1741 gctgtacagcttttctgtaagtataatcagactgtataaggggttttctatgagctagaag↓
1801 aattagccactaaaaagtttatttactggttagtatttatttctttaatacaatattccatt↓
1861 caccaaatgtgtagccgagcgacccccctataaagcatcgttttgtgtacttaaaatagag↓
1921 cactgggtgaaatgctaggaacctgattgtcttctgctatatccagacggagagatcagagg↓
1981 cgagttcaatggtctgcatcagcatgtgatttacatggteccaaaaattttgtttgttg↓
2041 ttaaataaaattttgaaacattccaacacccaaaaaaaccccccccccccccccccccccc#

```

Figure 1. Complete coding sequences and deduced protein sequences of BMP2 (A) and BMP4 (B). The conserved TGF-β propeptide and mature TGF-β domain are indicated by yellow and red shading, respectively. The signal peptide is marked with a green background, and the initiation codons (ATG) and termination codons (TGA) are underlined.

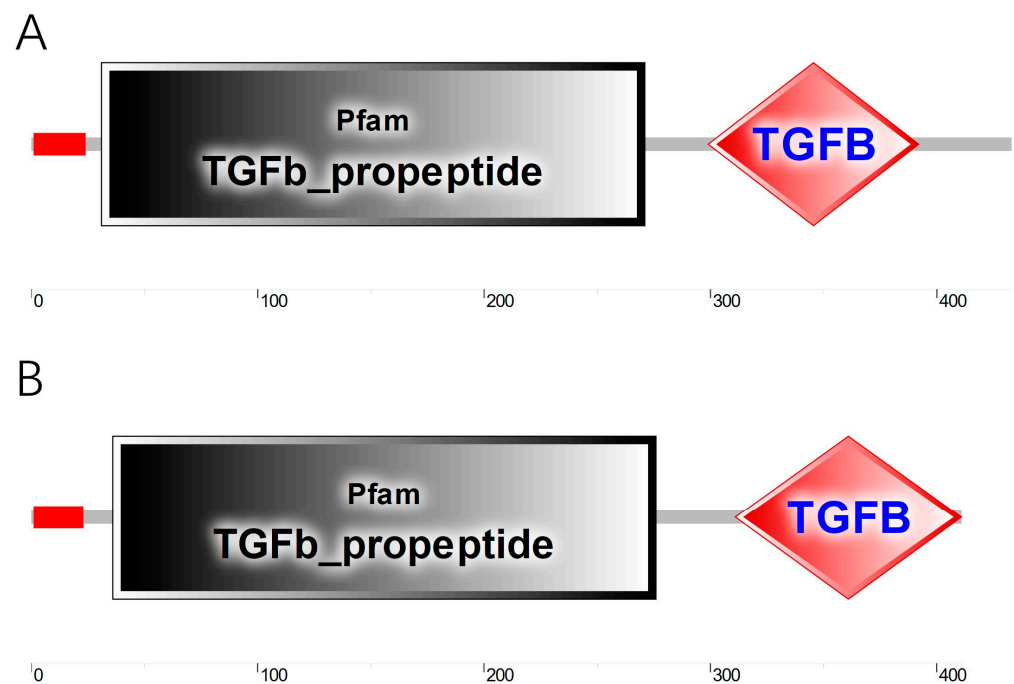


**Figure 2.** BMP2 (A) and BMP4 (B) domain structures in *C. auratus* red var. Three key structural features are shown, including a signal peptide (the first region marked in red), a TGF- $\beta$  propeptide, and a mature TGF- $\beta$  domain.

### 3.3. Expression Profiles of BMP2 and BMP4 in the Adult Fish

The expression patterns of *BMP2* and *BMP4* genes were detected in different tissues of adult *C. auratus* red var. fish by qRT-PCR. The findings revealed the widespread expression of *BMP2* and *BMP4* in all nine tissues examined: gill (G), caudal fin (C), heart (H), intestine (I), kidney (K), liver (L), muscle (M), brain (B), and spleen (S). Specifically, *BMP2* exhibited high expression levels in the muscle, gill, liver, and caudal fin, with lower expression in the heart. Moderate expression was observed in the brain, intestine, kidney, and spleen (Figure 6A). On the other hand, *BMP4* showed relatively high expression in muscle and the liver, followed by the caudal fin and brain, but lower expression in the gill, intestine, spleen, heart, and kidney (Figure 6B).

### 3.4. BMP2 and BMP4 Expression in Different Developmental Stages after NP Treatment

Under the NP treatment, abnormal tailbone formation was observed in embryos (Figure S1), which is consistent with the results of our group's previous research [30]. To investigate the effect of NP exposure on the expression of *BMP2* and *BMP4*, the levels of *BMP2* and *BMP4* mRNA were examined at six developmental stages of *C. auratus* red var. embryos, including 6 hpf, 12 hpf, 24 hpf, 48 hpf, 72 hpf, and 96 hpf (Figure 7). qRT-PCR analysis showed that the expressions of *BMP2* and *BMP4* in the 3  $\mu\text{mol/L}$  NP treatment group were significantly downregulated at 6 hpf, 12 hpf, and 96 hpf compared with the control group, and *BMP2* expression was also significantly decreased at 72 hpf ( $p < 0.05$ ). There were non-significant changes in the expression levels of *BMP2* at 24 hpf and 48 hpf and *BMP4* at 24 hpf, 48 hpf, and 72 hpf after the NP treatment ( $p > 0.05$ ).



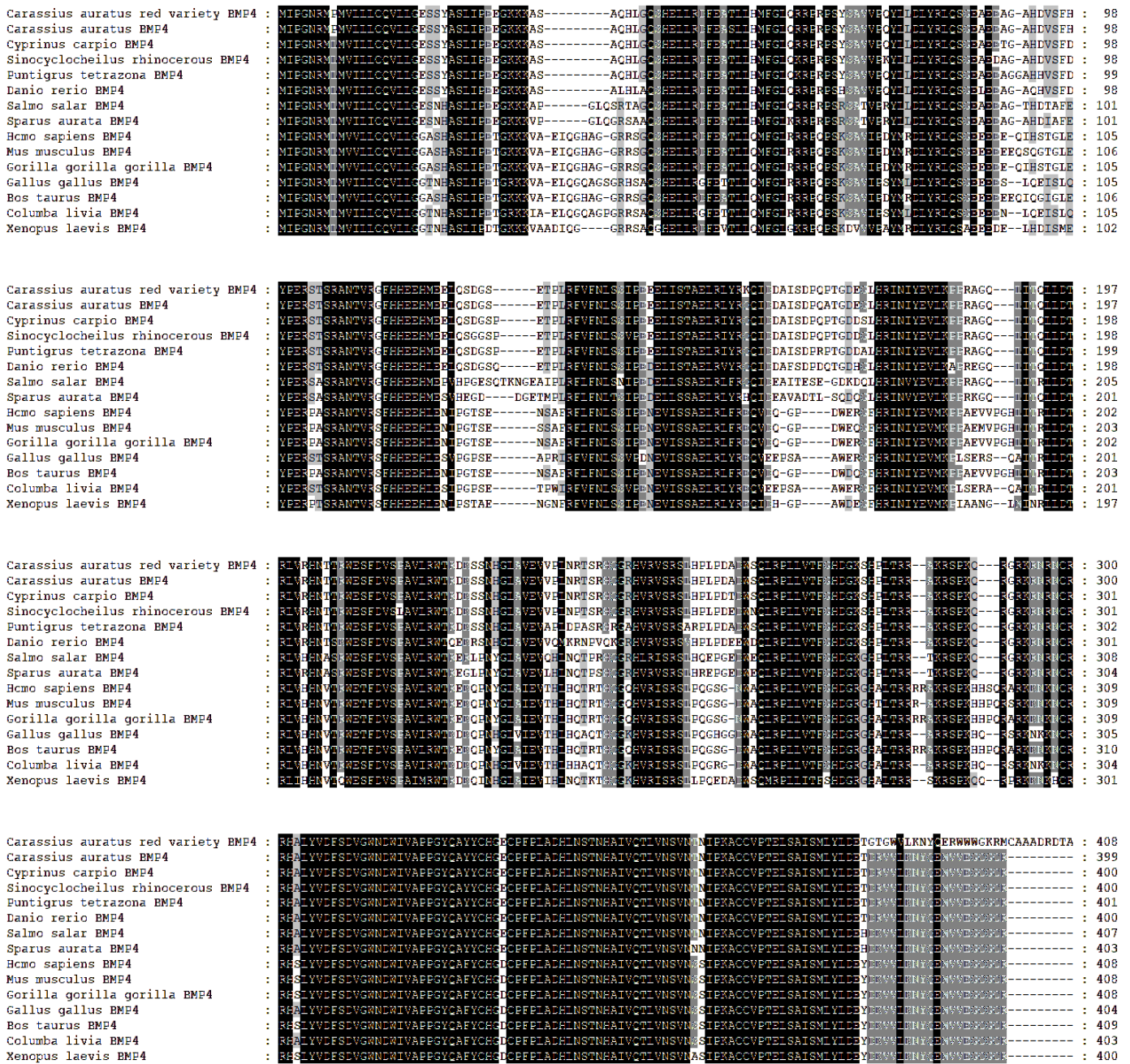
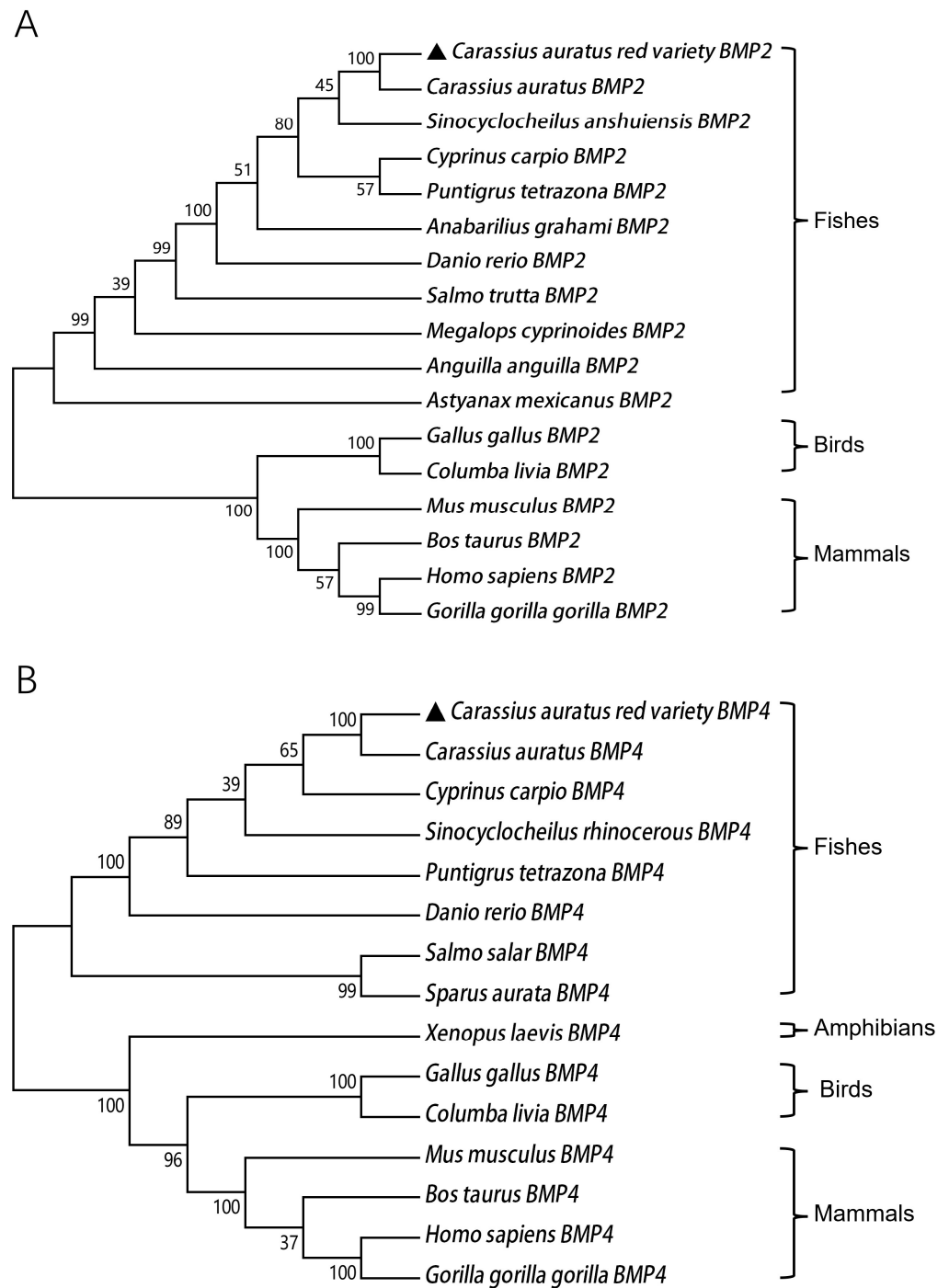
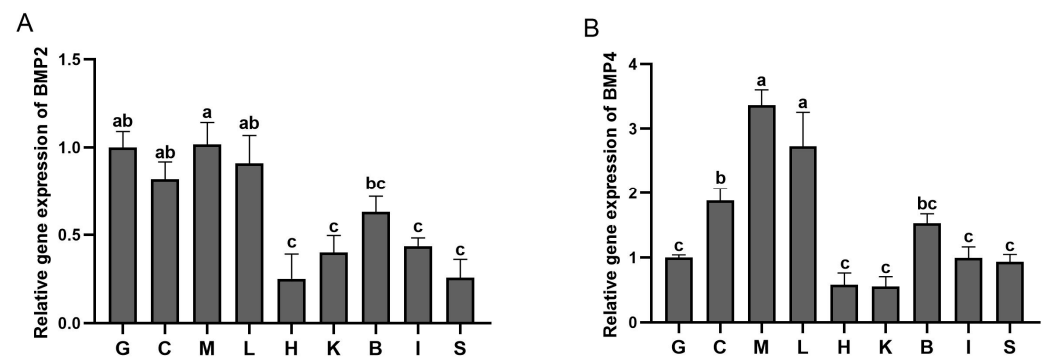


Figure 4. Multiple amino acid sequence alignment of BMP4 from *C. auratus* red var. and other species. The same amino acids are marked with black, and amino acids with more than 75% and 50% similarity are, respectively, shown in dark gray and light gray.



**Figure 5.** Phylogenetic tree of BMP2 (A) and BMP4 (B) sequences in different vertebrates (*C. auratus* red var. BMP2 and BMP4 are marked with black triangles). The phylogenetic tree was constructed using the neighbor-joining (NJ) algorithm. Node values represent the bootstrap values obtained after 1000 replications. The GenBank accession numbers of BMP2 and BMP4 are listed in Table 2.



**Figure 6.** Relative expression of *C. auratus* red var. *BMP2* and *BMP4* in the gill (G), caudal fin (C), heart (H), intestine (I), kidney (K), liver (L), muscle (M), brain (B), and spleen (S). Transcriptional fold-changes of *BMP2* and *BMP4* in different tissues were calculated compared to gill tissue, and  $\beta$ -actin was employed as the internal reference. Different lowercase letters represent significant differences ( $p < 0.05$ ,  $n = 3$ ).

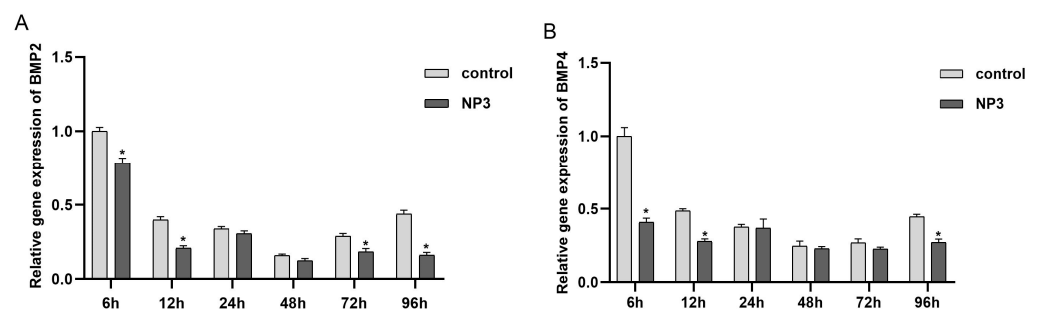


**Figure 7.** Expression levels of *BMP2* (A) and *BMP4* (B) in the treatment and control groups at six developmental stages of *C. auratus* red var. embryos (control: 0  $\mu\text{mol/L}$  NP-treated embryos; NP3: 3  $\mu\text{mol/L}$  NP-treated embryos).  $\beta$ -actin was used as the internal reference. Transcriptional fold-changes in the target gene at different time points were calculated compared with the control (6 h). Significant differences at different time points after NP exposure compared with corresponding control groups are indicated by asterisks (\*:  $p < 0.05$ ;  $n = 3$ ).

### 3.5. Impact of NP and LDN193189 on BMP-Smad Pathway Gene Expression

To assess the impact of NP exposure on *BMP2*, *BMP4*, and other BMP-Smad pathway-related genes, the expression levels of *BMPRI*, *BMP2*, *BMP4*, *Runx2*, and *Osterix* were quantified in the caudal fin of *C. auratus* red var. at 12, 24, 48, 72, and 96 h post-exposure (Figure 8). At 12 h, a significant upregulation of *BMPRI*, *BMP4*, and *Runx2* was observed under a low NP concentration ( $p < 0.05$ ), whereas *BMP2* expression was downregulated ( $p < 0.05$ ). At 24 h, under a low NP concentration, *BMPRI*, *BMP2*, *Runx2*, and *Osterix* mRNA levels were significantly increased ( $p < 0.05$ ). At 12 h under high NP exposure, *BMPRI* and *Runx2* mRNA expression increased significantly ( $p < 0.05$ ), whereas *BMP2* expression decreased ( $p < 0.05$ ). At 24 h, the expression of *BMPRI*, *BMP2*, and *Osterix* increased significantly under high NP exposure ( $p < 0.05$ ), while *BMP4* expression was significantly reduced ( $p < 0.05$ ). Expression of all genes analyzed progressively decreased with extended NP exposure time until 96 h, with the most significant differences observed at 48 h, where *BMPRI*, *BMP2*, *BMP4*, *Runx2*, and *Osterix* expression levels were significantly downregulated ( $p < 0.05$ ). These findings indicated that the 251.3  $\mu\text{g/L}$  NP exposure group exerted a more pronounced effect on the expression of the *BMPRI*, *BMP2*, *BMP4*, *Runx2*, and *Osterix* genes compared with the 753.9  $\mu\text{g/L}$  NP exposure group.

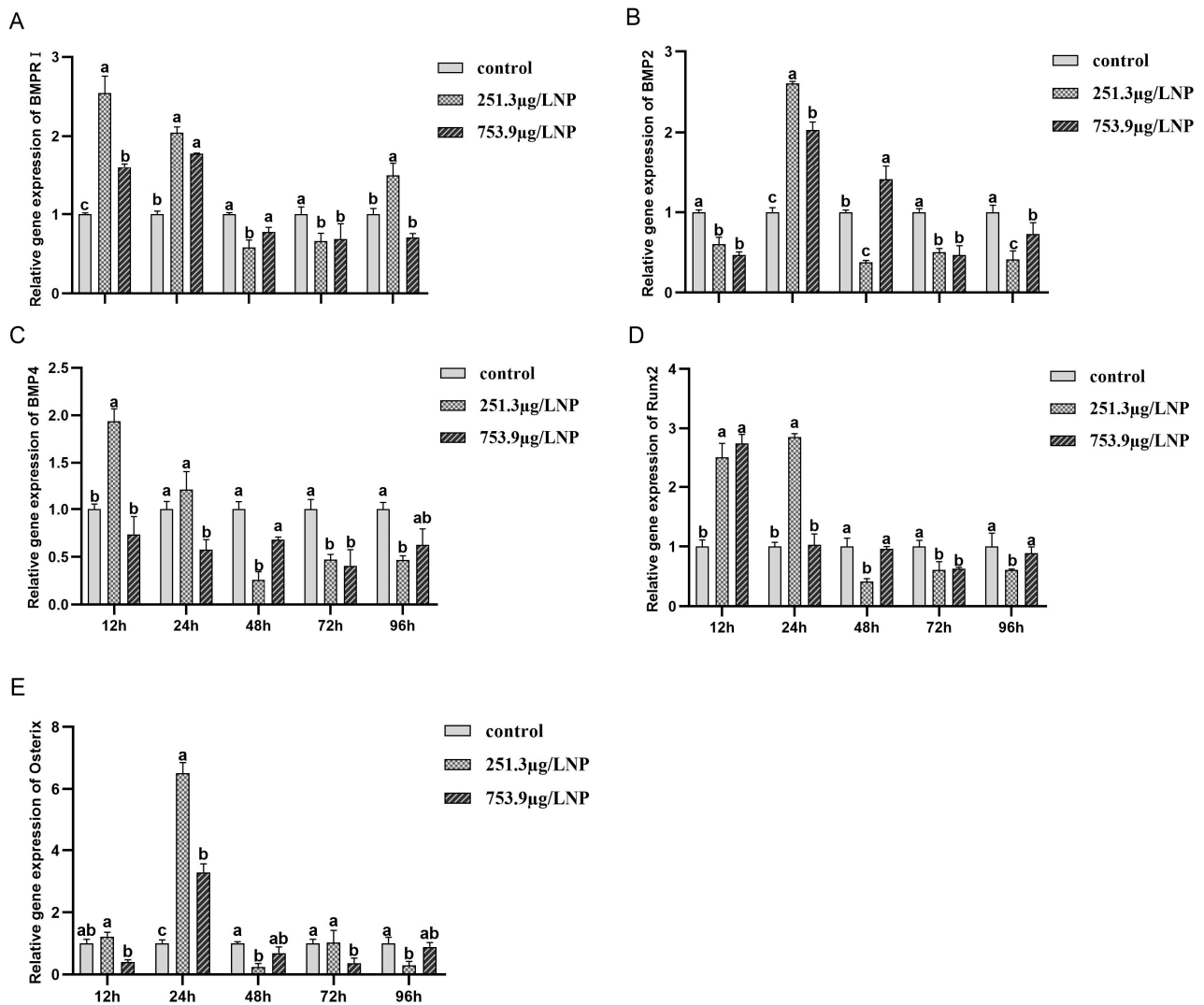


**Figure 8.** Effect of different concentrations of NP stress on the expression levels of *BMPRI* (A), *BMP2* (B), *BMP4* (C), *Runx2* (D), and *Osterix* (E) mRNA in caudal fin (0.01% ethanol-treated control group; 251.3 µg/L NP-treated group; 753.9 µg/L NP-treated group).  $\beta$ -actin was used as the internal reference. The transcriptional fold-changes in the target genes were calculated compared with the corresponding control group. Statistically significant differences ( $p < 0.05$ ) are indicated by different lowercase letters.

To further elucidate the effects of NP stress on BMP-Smad pathway-related gene expression, adult fish were treated with the specific *BMPRI* inhibitor LDN193189 followed by combined NP exposure. After a 12 h injection with LDN193189, fish were then exposed to 251.3 µg/L of NP for an additional 48 h. The results revealed that LDN193189 significantly decreased the activity of *BMPRI*, *BMP2*, *BMP4*, *Runx2*, and *Osterix* ( $p < 0.05$ ). In comparison with the control group, the combined treatment with LDN193189 and NP led to a greater reduction in the expression levels of *BMPRI*, *BMP2*, *BMP4*, *Runx2*, and *Osterix* than either treatment alone (Figure 9).

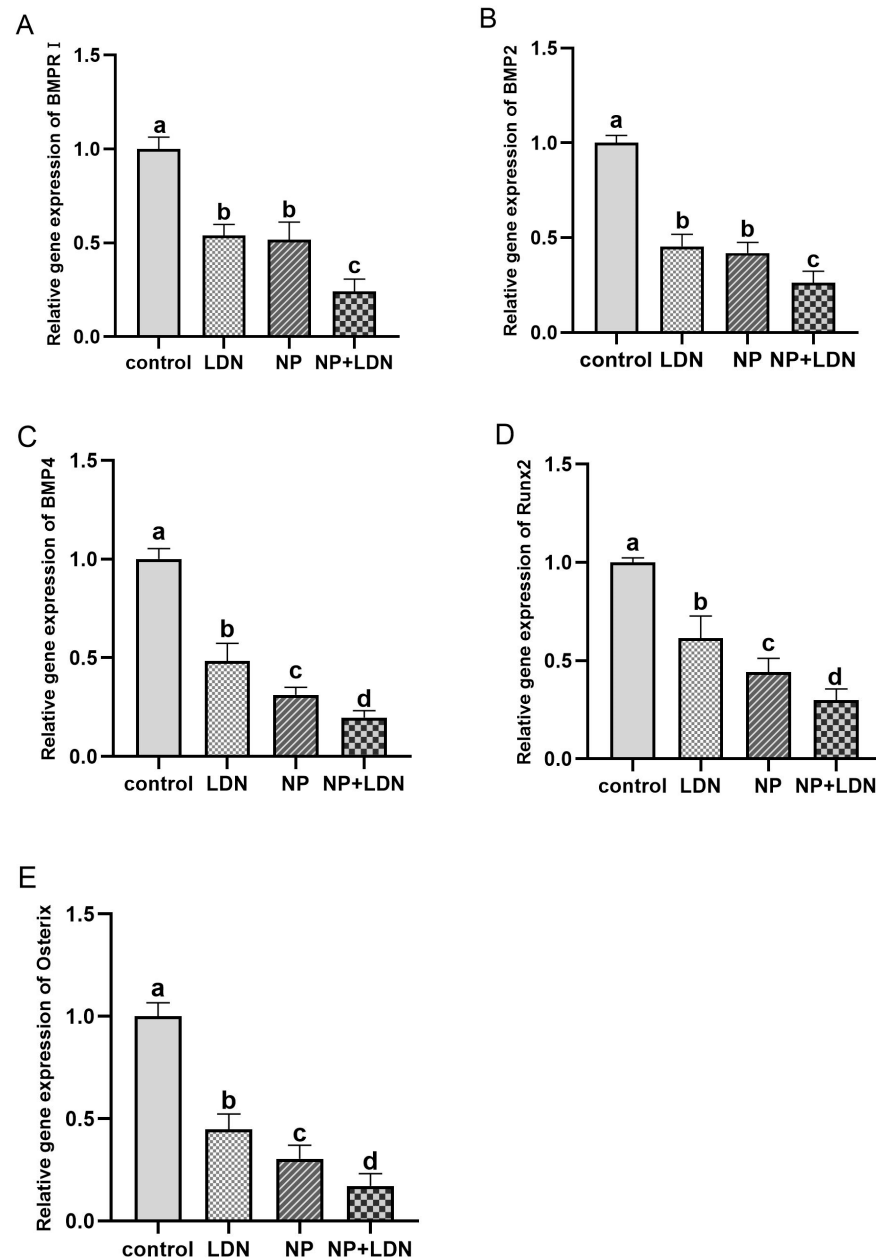


**Figure 9.** Effects of NP exposure and LDN193189 injection on the relative expression of *BMPRI* (A), *BMP2* (B), *BMP4* (C), *Runx2* (D), and *Osterix* (E) mRNA in caudal fin of *C. auratus* red var. Control: exposed to 0.01% ethanol and injected with 0.01% DMSO; LDN: injected with 0.625 mg/kg LDN193189 and exposed to 0.01% ethanol; NP: injected with 0.01% DMSO and exposed to 251.3  $\mu\text{g/L}$  NP; NP+LDN: injected with 0.625 mg/kg LDN193189 and exposed to 251.3  $\mu\text{g/L}$  NP.  $\beta$ -actin was used as the internal reference. Transcriptional fold-changes in target gene were calculated compared with the control. The different lowercase letters indicate statistically significant differences ( $p < 0.05$ ).

#### 4. Discussion

The bone morphogenetic protein (BMP) family plays a crucial role in regulating cellular activities and is involved in almost all tissue development processes [33,34]. BMPs are essential for bone formation during mammalian development and exhibit diverse functions within the body [35]. Disruptions of TGF- $\beta$ /BMP signaling have been implicated in multiple bone diseases [36]. In this study, the BMP2 and BMP4 of *C. auratus* red var. contained seven conserved cysteine residues, which are typical features of the BMP family [37]. Protein domain analysis revealed both the BMP2 and BMP4 proteins of *C. auratus* red

var. possessed two TGF- $\beta$  domains, which is a mature peptide that controls proliferation, differentiation, and other functions in many cell types [38]. Multiple alignments of the vertebrate BMP2 and BMP4 protein sequences available revealed the high conservation of amino acid residues. Phylogenetic analysis showed that the amino acid sequences of BMP2 and BMP4 were conserved among the analyzed fish species, and *C. auratus* red var. sequences were closely related to those of *C. auratus*. The structure and sequence similarity of BMP2 and BMP4 between *C. auratus* red var. and other fish suggests that cloned *C. auratus* red var. BMPs belong to the teleost BMP family.

Research has indicated that the *BMP2* and *BMP4* genes are broadly expressed across various tissues in fish, with expression patterns exhibiting species-specific variability. For instance, in *C. carpio*, both the *BMP2* and *BMP4* genes are expressed at high levels in several healthy tissues, including the gill, intestine, liver, spleen, brain, and blood [39]. In *C. carpio* var. Jian, the expression of *BMP2* is most highly expressed in muscle, with subsequent levels observed in the liver; however, lower expression levels have been detected in both the heart and brain [26]. In barbel steed (*Hemibarbus labeo*), *BMP2* shows preferential expression in the gill, with significant levels also detected in muscle and the liver, while expression in the heart is lower [27]. In the current study, qRT-PCR was employed to assess the expression of *BMP2* and *BMP4* in various tissues of *C. auratus* red var. Expression was detected in all sampled tissues, with the muscle and liver exhibiting higher levels, followed by the caudal fin and lower levels in the heart. This widespread distribution suggests diverse physiological roles for *BMP2* and *BMP4* in *C. auratus* red var. For example, higher expression in muscle suggests that *BMP2* and *BMP4* might be related to the occurrence of intramuscular spines [26]. In the liver, their higher expression indicates the importance of the BMP pathway in liver development, where it is closely related to iron balance in the liver [27,40]. High expression in the caudal fin suggests that *BMP2* and *BMP4* are involved in the process of bone formation [41]. Comparatively, the tissue-specific expression pattern in *C. auratus* red var. closely aligns with that observed in *Cyprinus carpio* var. Jian, another cyprinid species. This conservation of expression patterns within cyprinids suggests that *BMP2* and *BMP4* may play evolutionarily conserved roles in these fishes, with potential implications for understanding their physiological functions across different tissues.

Nonylphenol (NP) has been examined for its toxicological effects across multiple tissues, with particular emphasis on the skeletal system [4,6]. It has been demonstrated that NP plays a critical role in bone, which can inhibit osteoclast formation and lead to skeletal disorders [42]. Furthermore, NP may modulate the molecular mediators involved in osteoblast differentiation through its interaction with estrogen receptors [43]. The BMP signaling pathways are known to be important in osteoblast differentiation [17]. This suggests that NP may influence BMP pathway-related genes through its interaction with estrogen receptors. As prominent ligands of this pathway, *BMP2* and *BMP4* activate it by binding to BMP type I (BMPRI) and type II (BMPRII) receptors, triggering the phosphorylation of downstream proteins such as Smad1/5/8 [44]. Subsequently, the phosphorylated Smad complex with Smad4 translocates to the nucleus and acts as a transcription factor, regulating genes such as *Runx2* and *Osterix*, which are crucial for bone formation and maintenance [45]. In our study, we found that NP exposure can significantly depress the expression of *BMP2* and *BMP4* in *C. auratus* red var. embryos and adults. BMP plays a crucial role in the formation of the body axis, particularly in the development of the ventral side during early life stages [46]. NP's effects on embryos can lead to the downregulation of *BMP2* and *BMP4* expression, resulting in morphological changes such as the abnormal development of tail bones during the early life stages [30]. In addition, in the cotreatment group, an intraperitoneal injection of the BMPRI-specific inhibitor LDN193189 was administered to disrupt gene expression, along with exposure to 251.3  $\mu\text{g}/\text{L}$  of NP; the expression levels of *BMPRI*, *BMP2*, *BMP4*, *Runx2*, and *Osterix* were downregulated more than in the other treatment groups. To date, there has been limited research exploring the effect of NP on the BMP-Smad signaling pathway in fish. Our results align with those of previous research, which has demonstrated that 2.5  $\mu\text{M}$  of NP reduces the expression

of BMPs during the osteogenic differentiation of mesenchymal stem cells into osteoblasts in rats [47]. The results suggest that NP may inhibit osteoclast formation by interfering with the expression of BMP pathway-related genes, which will provide cues for further research on the molecular mechanism of the NP effect on bone development. Studies of gobiid fish (*Odontobutis potamophila*) have shown that long-term exposure to NP can affect the tissue structure of the testes, leading to cell necrosis and fibrosis [48]. In this study, an acute exposure experiment was conducted that does not provide a thorough understanding of the effects of long-term NP exposure on fish.

Recent studies have increasingly uncovered the potential hazards of endocrine-disrupting chemicals (EDCs) on the skeletal development of aquatic organisms. Evidence suggests that EDCs can inhibit the expression of key skeletal development genes, such as *BMP2*, *BMP4*, *Sox9*, and *Runx2*. This study further validates these findings by experimentally observing that NP, a ubiquitous EDC, significantly reduces the expression levels of the *BMP2* and *BMP4* genes in *Carassius auratus* red var. This discovery is consistent with the inhibitory effects observed previously in other fish exposed to EDCs, such as bisphenol A (BPA) [49] and benzyl butyl phthalate (BBP) [50]. These findings underscore the crucial role of the BMP-Smad signaling pathway in the adaptive mechanisms of teleost fish in response to environmental toxicants. Concurrently, they highlight the significance of safeguarding aquatic ecosystems against EDC pollution. Hence, this research establishes a scientific framework for the formulation of environmental management strategies that specifically target EDCs, aiming to alleviate their potential detrimental effects on aquatic organisms and ecological systems.

## 5. Conclusions

In the present study, full-length cDNAs of BMP2 and BMP4 were successfully isolated and characterized from *Carassius auratus* red var. Homology and phylogenetic analyses indicated that BMP2 and BMP4 were most closely related to BMP2 and BMP4 from *C. auratus* and were relatively conservative between different species. Furthermore, tissue-specific distributions showed that these two proteins were expressed in all tissues examined and highly expressed in muscle, the liver, and the caudal fin. The levels of BMP2 and BMP4 mRNA were downregulated at different developmental stages of embryos after NP exposure. Additionally, the different concentrations of NP stress on the caudal fins of adult fish affected the expression of BMP2, BMP4, and other BMP-Smad pathway-related genes. Importantly, the results of the independent and combined treatments with NP and the BMPRI specific inhibitor suggested that NP reduced the expression of BMPRI, BMP2, BMP4, Runx2, and Osterix. Our findings demonstrate that BMP2 and BMP4 may play a regulatory role via the BMP-Smad pathway under the exposure of NP and advance our understanding of how NP stress affects BMP2 and BMP4.

**Supplementary Materials:** The following supporting information can be downloaded at: <https://www.mdpi.com/article/10.3390/fishes9050159/s1>, Figure S1: Morphological changes of the *Carassius auratus* red var. embryos at different developmental stages exposed to NP exposure; Table S1: Embryo sampling details for NP exposure experiments.

**Author Contributions:** Y.S. and X.C. conceived and designed the study. D.L., S.C., J.X. and Y.L. performed the experiments. D.L. and Q.Z. analyzed the data and discussed the main findings. D.L., Q.Z. and Y.S. wrote and revised the manuscript. All authors have read and agreed to the published version of the manuscript.

**Funding:** This research was funded by the Scientific Research Fund of the Hunan Provincial Education Department (Grant No. 21B0923) and the Postgraduate Scientific Research Innovation Project of Hunan Province (Grant No. CX20221061).

**Institutional Review Board Statement:** The study was approved by the Animal Ethical Review Committee (AERC) of Hunan Normal University (Approval code: 20221013009; Approval date: 20 October 2022) and followed the guidelines statement of the Administration of Affairs Concerning Animal Experimentation of China. This manuscript does not involve the use of any human data or

tissue. The animals used in this study came from Hunan Normal University, and we obtained written consent from Hunan Normal University to use these animals in our research.

**Informed Consent Statement:** Not applicable.

**Data Availability Statement:** The datasets used and/or analyzed during the current study are available from the corresponding author on reasonable request.

**Acknowledgments:** We thank the laboratory members for their technical assistance and constructive comments.

**Conflicts of Interest:** The authors declare no conflicts of interest.

## References

- Nishie, T.; Komaru, A.; Shiroguchi, S.; Yamaizumi, T.; Ono, Y.; Motomochi, A.; Tooyama, I.; Fujioka, Y.; Sakai, N.; Higaki, S.; et al. Nonylphenol reduced the number of haploids in in vitro spermatogenesis of the endangered cyprinid *Gnathopogon caeruleus*. *Toxicol. Vitro*. **2023**, *89*, 105565. [[CrossRef](#)] [[PubMed](#)]
- Hart, C.E.; Lauth, M.J.; Hunter, C.S.; Krasny, B.R.; Hardy, K.M. Effect of 4-nonylphenol on the immune response of the pacific oyster *Crassostrea gigas* following bacterial infection with *Vibrio campbellii*. *Fish. Shellfish. Immunol.* **2016**, *58*, 449–461. [[CrossRef](#)] [[PubMed](#)]
- Xia, Y.Y.; Zhan, P.; Wang, Y. Effects of nonylphenol on brain gene expression profiles in F1 generation rats. *Biomed. Environ. Sci.* **2008**, *21*, 1–6. [[CrossRef](#)] [[PubMed](#)]
- Ni, C.; Pan, K.; Xu, J.; Long, X.; Lin, F.; Nie, Y.; Yang, Y.; Yu, J. Effects and mechanism of perinatal nonylphenol exposure on cardiac function and myocardial mitochondria in neonatal rats. *Ecotoxicol. Environ. Saf.* **2023**, *258*, 114977. [[CrossRef](#)] [[PubMed](#)]
- Suna, P.A.; Cengiz, O.; Ceyhan, A.; Atay, E.; Ertekin, T.; Nisari, M.; Yay, A. The protective role of curcumin against toxic effect of nonylphenol on bone development. *Hum. Exp. Toxicol.* **2021**, *40*, S63–S76. [[CrossRef](#)] [[PubMed](#)]
- Agas, D.; Sabbieti, M.G.; Marchetti, L. Endocrine disruptors and bone metabolism. *Arch. Toxicol.* **2013**, *87*, 735–751. [[CrossRef](#)] [[PubMed](#)]
- Miyawaki, J.; Kamei, S.; Sakayama, K.; Yamamoto, H.; Masuno, H. 4-tert-octylphenol regulates the differentiation of C3H10T1/2 cells into osteoblast and adipocyte lineages. *Toxicol. Sci.* **2008**, *102*, 82–88. [[CrossRef](#)] [[PubMed](#)]
- Zhong, Z.; Ethen, N.J.; Williams, B.O. Wnt signaling in bone development and homeostasis. *Wiley Interdiscip. Rev. Dev. Biol.* **2014**, *3*, 489–500. [[CrossRef](#)] [[PubMed](#)]
- Mukherjee, U.; Samanta, A.; Biswas, S.; Ghosh, S.; Das, S.; Banerjee, S.; Maitra, S. Chronic exposure to nonylphenol induces oxidative stress and liver damage in male zebrafish (*Danio rerio*): Mechanistic insight into cellular energy sensors, lipid accumulation and immune modulation. *Chem. Biol. Interact.* **2022**, *351*, 109762. [[CrossRef](#)]
- Desai, J.K.; Trangadia, B.J.; Patel, U.D.; Patel, H.B.; Kalaria, V.A.; Kathiriya, J.B. Neurotoxicity of 4-nonylphenol in adult zebrafish: Evaluation of behaviour, oxidative stress parameters and histopathology of brain. *Environ. Pollut.* **2023**, *334*, 122206. [[CrossRef](#)]
- Horie, Y.; Kanazawa, N.; Takahashi, C.; Tatarazako, N.; Iguchi, T. Gonadal soma-derived factor expression is a potential biomarker for predicting the effects of endocrine-disrupting chemicals on gonadal differentiation in Japanese medaka (*Oryzias latipes*). *Environ. Toxicol. Chem.* **2022**, *41*, 1875–1884. [[CrossRef](#)] [[PubMed](#)]
- Chaube, R.; Gautam, G.J.; Joy, K.P. Teratogenic effects of 4-nonylphenol on early embryonic and larval development of the catfish *Heteropneustes fossilis*. *Arch. Environ. Contam. Toxicol.* **2013**, *64*, 554–561. [[CrossRef](#)] [[PubMed](#)]
- Zhang, H.; Jiang, J.L.; Shan, Z.J.; Bu, Y.Q.; Tian, F. Toxic effects of 4-nonylphenol on embryo/larva of zebrafish (*Danio rerio*). *J. Ecol. Rural. Environ.* **2017**, *33*, 737–742. [[CrossRef](#)]
- Zhang, Q.Y.; Sun, Y.D.; Wang, Z.J.; Hu, X.J.; Kui, X. Preliminary study on toxicity of nonylphenol to embryo development of goldfish (*Carassius auratus*). *Prog. Mod. Biomed.* **2016**, *16*, 3040–3043. [[CrossRef](#)]
- Shu, B.; Zhang, M.; Xie, R.; Wang, M.; Jin, H.; Hou, W.; Tang, D.; Harris, S.E.; Mishina, Y.; O’Keefe, R.J.; et al. BMP2, but not BMP4, is crucial for chondrocyte proliferation and maturation during endochondral bone development. *J. Cell Sci.* **2011**, *124*, 3428–3440. [[CrossRef](#)] [[PubMed](#)]
- Yoon, B.S.; Lyons, K.M. Multiple functions of BMPs in chondrogenesis. *J. Cell Biochem.* **2004**, *93*, 93–103. [[CrossRef](#)] [[PubMed](#)]
- Wan, M.; Cao, X. BMP signaling in skeletal development. *Biochem. Biophys. Res. Commun.* **2005**, *328*, 651–657. [[CrossRef](#)] [[PubMed](#)]
- Salazar, V.S.; Gamer, L.W.; Rosen, V. BMP signalling in skeletal development, disease and repair. *Nat. Rev. Endocrinol.* **2016**, *12*, 203–221. [[CrossRef](#)] [[PubMed](#)]
- Hwang, J.K.; Min, K.H.; Choi, K.H.; Hwang, Y.C.; Jeong, I.K.; Ahn, K.J.; Chung, H.Y.; Chang, J.S. Bisphenol A reduces differentiation and stimulates apoptosis of osteoclasts and osteoblasts. *Life Sci.* **2013**, *93*, 367–372. [[CrossRef](#)]
- Ju, L.; Tang, K.; Guo, X.R.; Yang, Y.; Zhu, G.Z.; Lou, Y. Effects of embryonic exposure to polychlorinated biphenyls on zebrafish skeletal development. *Mol. Med. Rep.* **2012**, *5*, 1227–1231. [[CrossRef](#)]
- Bandyopadhyay, A.; Tsuji, K.; Cox, K.; Harfe, B.D.; Rosen, V.; Tabin, C.J. Genetic analysis of the roles of BMP2, BMP4, and BMP7 in limb patterning and skeletogenesis. *PLoS Genet.* **2006**, *2*, e216. [[CrossRef](#)] [[PubMed](#)]
- Li, X.K.; Huang, Q.K.; Feng, L.L.; Guo, Y.F.; Liang, J.; Lan, G.Q. Sequence and expression differences of BMP2 and FGFR3 genes in Guangxi bama mini pig and landrace pig. *J. South. Agric.* **2021**, *52*, 1709–1718. [[CrossRef](#)]
- Li, M.; Liu, X.; Liu, X.; Ge, B. Calcium phosphate cement with BMP-2-loaded gelatin microspheres enhances bone healing in osteoporosis: A pilot study. *Clin. Orthop. Relat. Res.* **2010**, *468*, 1978–1985. [[CrossRef](#)] [[PubMed](#)]

24. Martínez-Barberá, J.P.; Toresson, H.; Da Rocha, S.; Krauss, S. Cloning and expression of three members of the zebrafish BMP family: BMP2A, BMP2B and BMP4. *Gene* **1997**, *198*, 53–59. [[CrossRef](#)] [[PubMed](#)]
25. Zeng, X.; Shi, Z.Y.; Chen, X.W.; Cheng, Q.Q. Skeleton development of Japanese flounder (*Paralichthys solivaceus*) and expression analysis of related genes (SOX9, BMP4 and BMP2) during metamorphosis. *Mar. Fish.* **2009**, *31*, 337–346. [[CrossRef](#)]
26. Ma, L.X.; Dong, Z.J.; Su, S.Y.; Zhang, J.Q.; Liu, W.; Li, L.L.; Yuan, X.H. Cloning of fragments of bone morphogenetic protein gene (BMP2B) of *Cyprinus carpio* var. Jian and its expression analysis. *Jiangsu J. Agr. Sci.* **2013**, *29*, 370–378. [[CrossRef](#)]
27. Chen, J.; Lü, Y.P.; Dai, Q.M.; Zhang, L.; Xu, C.B.; Lu, J. Molecular characterization of a BMP2A homologue in barbel steed (*Hemibarbus labeo*) and its involvement in intermuscular bone development. *Acta Hydrobiol. Sin.* **2021**, *45*, 8–13. [[CrossRef](#)]
28. Cao, X.Y.; Ma, C.X.; Xia, X.; Zhang, R.Q.; Chen, X.W.; Zhao, J.L. Cloning and expression analysis of jaw remodeling developmental gene BMP4 in *Siniperca chuatsi*. *Genom. Appl. Biol.* **2020**, *39*, 5075–5083. [[CrossRef](#)]
29. Huang, L.; Deng, X.; Yang, X.; Tang, Z.; Fan, S.; Zhou, Z.; Tao, M.; Liu, S. Cloning, distribution, and effects of growth regulation of MC3R and MC4R in red crucian carp (*Carassius auratus* red var.). *Front. Endocrinol.* **2024**, *14*, 1310000. [[CrossRef](#)]
30. Tian, Y.S.; Sun, Y.D.; Ou, M.; Liu, Y.F.; Cui, X.J.; Zhou, D.G.; Che, W.A.; Chen, K.C. Preliminary studies on the mechanism of nonylphenol-induced malformation of *Carassius auratus* red var. *J. Fish. China* **2020**, *44*, 1619–1636. [[CrossRef](#)]
31. Lu, X.H.; Gu, Y.; Song, Y. Toxicity and tissue accumulation of nonylphenol in *Carassius auratus* red variety, Grass Carp and Sliver Carp. *J. Hyg. Res.* **2012**, *41*, 785–789. [[CrossRef](#)]
32. Rajaram, S.; Patel, S.; Uggini, G.K.; Desai, I.; Balakrishnan, S. BMP signaling regulates the skeletal and connective tissue differentiation during caudal fin regeneration in sailfin molly (*Poecilia latipinna*). *Dev. Growth Differ.* **2017**, *59*, 629–638. [[CrossRef](#)] [[PubMed](#)]
33. Schlange, T.; André, B.; Arnold, H.H.; Brand, T. BMP2 is required for early heart development during a distinct time period. *Mech. Dev.* **2000**, *91*, 259–270. [[CrossRef](#)] [[PubMed](#)]
34. Du, Y.; Xiao, Q.; Yip, H.K. Regulation of retinal progenitor cell differentiation by bone morphogenetic protein 4 is mediated by the smad/id cascade. *Invest. Ophthalmol. Vis. Sci.* **2010**, *51*, 3764–3773. [[CrossRef](#)] [[PubMed](#)]
35. Katagiri, T.; Takahashi, N. Regulatory mechanisms of osteoblast and osteoclast differentiation. *Oral. Dis.* **2002**, *8*, 147–159. [[CrossRef](#)]
36. Miyazono, K.; Maeda, S.; Imamura, T. BMP receptor signaling: Transcriptional targets, regulation of signals, and signaling cross-talk. *Cytokine Growth Factor. Rev.* **2005**, *16*, 251–263. [[CrossRef](#)] [[PubMed](#)]
37. Bragdon, B.; Moseychuk, O.; Saldanha, S.; King, D.; Julian, J.; Nohe, A. Bone morphogenetic proteins: A critical review. *Cell Signal.* **2011**, *23*, 609–620. [[CrossRef](#)] [[PubMed](#)]
38. Hinck, A.P.; Archer, S.J.; Qian, S.W.; Roberts, A.B.; Sporn, M.B.; Weatherbee, J.A.; Tsang, M.L.; Lucas, R.; Zhang, B.L.; Wenker, J.; et al. Transforming growth factor beta 1: Three-dimensional structure in solution and comparison with the X-ray structure of transforming growth factor beta 2. *Biochemistry* **1996**, *35*, 8517–8534. [[CrossRef](#)] [[PubMed](#)]
39. Chen, L.; Dong, C.; Kong, S.; Zhang, J.; Li, X.; Xu, P. Genome wide identification, phylogeny, and expression of bone morphogenetic protein genes in tetraploidized common carp (*Cyprinus carpio*). *Gene* **2017**, *627*, 157–163. [[CrossRef](#)]
40. Shin, D.; Shin, C.H.; Tucker, J.; Ober, E.A.; Rentzsch, F.; Poss, K.D.; Hammerschmidt, M.; Mullins, M.C.; Stainier, D.Y. Bmp and Fgf signaling are essential for liver specification in zebrafish. *Development* **2007**, *134*, 2041–2050. [[CrossRef](#)]
41. Rafael, M.S.; Laizé, V.; Cancela, M.L. Identification of *Sparus aurata* bone morphogenetic protein 2: Molecular cloning, gene expression and in silico analysis of protein conserved features in vertebrates. *Bone* **2006**, *39*, 1373–1381. [[CrossRef](#)]
42. Hagiwara, H.; Sugizaki, T.; Tsukamoto, Y.; Senoh, E.; Goto, T.; Ishihara, Y. Effects of alkylphenols on bone metabolism in vivo and in vitro. *Toxicol. Lett.* **2008**, *181*, 13–18. [[CrossRef](#)] [[PubMed](#)]
43. Sabbieti, M.G.; Agas, D.; Palermo, F.; Mosconi, G.; Santoni, G.; Amantini, C.; Farfariello, V.; Marchetti, L. 4-nonylphenol triggers apoptosis and affects 17- $\beta$ -estradiol receptors in calvarial osteoblasts. *Toxicology* **2011**, *290*, 334–341. [[CrossRef](#)] [[PubMed](#)]
44. Nohe, A.; Hassel, S.; Ehrlich, M.; Neubauer, F.; Sebald, W.; Henis, Y.I.; Knaus, P. The mode of bone morphogenetic protein (BMP) receptor oligomerization determines different BMP-2 signaling pathways. *J. Biol. Chem.* **2002**, *277*, 5330–5338. [[CrossRef](#)]
45. Bruderer, M.; Richards, R.G.; Alini, M.; Stoddart, M.J. Role and regulation of RUNX2 in osteogenesis. *Eur. Cell Mater.* **2014**, *28*, 269–286. [[CrossRef](#)]
46. Wu, Y.; Sun, A.; Nie, C.; Gao, Z.X.; Wan, S.M. Functional differentiation of BMP2A and BMP2B genes in zebrafish. *Gene Expr. Patterns* **2022**, *46*, 119288. [[CrossRef](#)]
47. Hussein, A.M.; Sina, M. p-Nonylphenol impairment of osteogenic differentiation of mesenchymal stem cells was found to be due to oxidative stress and down-regulation of RUNX2 and BMP. *Endocr. Metab. Immune Disord. Drug Targets.* **2020**, *20*, 1336–1346. [[CrossRef](#)] [[PubMed](#)]
48. Li, X.J.; Zhou, Z.L.; Gu, J.H. Effect of nonylphenol on the gonadal differentiation and development in gobbid fish (*Odontobutis potamophila*). *Fish. Sci.* **2009**, *28*, 15–19. [[CrossRef](#)]
49. Fan, X.; Wu, L.; Hou, T.; He, J.; Wang, C.; Liu, Y.; Wang, Z. Maternal bisphenol A exposure impaired endochondral ossification in craniofacial cartilage of rare minnow (*Gobiocypris rarus*) offspring. *Ecotoxicol. Environ. Saf.* **2018**, *163*, 514–520. [[CrossRef](#)]
50. Pu, S.Y.; Hamid, N.; Ren, Y.W.; Pei, D.S. Effects of phthalate acid esters on zebrafish larvae: Development and skeletal morphogenesis. *Chemosphere* **2020**, *246*, 125808. [[CrossRef](#)]

**Disclaimer/Publisher’s Note:** The statements, opinions and data contained in all publications are solely those of the individual author(s) and contributor(s) and not of MDPI and/or the editor(s). MDPI and/or the editor(s) disclaim responsibility for any injury to people or property resulting from any ideas, methods, instructions or products referred to in the content.